Propane Pyrolysis Facilitated by Phenyl Radicals: A Combined Experimental and Kinetic Modeling Study

Peng Yu[a] and Hsi-Wu Wong[a]*

[a]Department of Chemical Engineering, University of Massachusetts Lowell
One University Avenue, Lowell, MA, 01854, USA

Abstract

Phenyl radicals generated from nitrobenzene were introduced as a hydrogen abstraction agent to accelerate propylene formation from propane pyrolysis. Neat propane pyrolysis and propane pyrolysis facilitated by phenyl radicals were carried out between 550 ºC and 650 ºC. Our experiments showed that phenyl facilitated pyrolysis gave higher propane conversion over neat reactions, with yields of all main products increased. However, propylene selectivity in phenyl facilitated pyrolysis decreased in favor of methane and ethylene. Detailed kinetic modeling shows that the formation of normal propyl and isopropyl radicals was accelerated due to increased hydrogen abstraction of propane by phenyl radicals. Decreased propylene selectivity in phenyl facilitated pyrolysis was resulted from the increased rates of secondary reactions converting propane and propylene into ethylene and methane. Our work demonstrates that a suitable free radical could facilitate propane pyrolysis for higher propylene yields. However, the balance between propylene yields and selectivity remains a major challenge.

Keywords: propane pyrolysis; phenyl radicals; olefin production; kinetic modeling; hydrogen abstraction

*Corresponding author: Hsi-Wu Wong, +1 (978) 954-5290, Email: hsiwu_wong@uml.edu

1 Introduction

Access to new supply of light alkanes (methane, ethane, propane, and butane) from shale deposits is one of the most exciting developments in the United States during the past decade (Kerr, 2010; Stevens, 2012; Wang et al., 2014). The relative abundance and low price of shale-derived alkanes gives the U.S. manufacturers a decisive competitive edge over other countries for petrochemical production (National Academies of Sciences and Medicine, 2016). This shale evolution also initiates a shift of ethylene production from oil-based naphtha to shale-derived ethane (Sattler et al., 2014b). The fact that ethane-based steam cracking reactors are more inexpensive to build and more efficient to operate than their naphtha-based counterparts also accelerates this shift. Ethane cracking, however, produces very little propylene. Typical propylene to ethylene production ratio from ethane cracking is 0.02 in mass, as opposed to 0.5 from traditional naphtha cracking (Wittcoff et al., 2004). Consequently, the shift from oil-derived naphtha to shale-derived ethane for ethylene production results in a growing gap of propylene demand.

Several on-purpose propylene (OPP) technologies have been developed to overcome this challenge (Bruijnincx and Weckhuysen, 2013). The most common OPP technology is propane dehydrogenation (PDH), in which propane is catalytically dehydrogenated to produce propylene and hydrogen (Nawaz, 2015). The major research effort on PDH has focused on finding an optimal catalyst to increase propylene yields, propylene selectivity, and catalyst lifetime (Deng et al., 2014; Sattler et al., 2014a; Schweitzer et al., 2014; Zhang et al., 2014). Two families of catalysts have shown the best promise: (1) supported platinum catalysts (Lee et al., 2014; Sattler et al., 2014c), and (2) chromium oxide catalysts (Jibril, 2004; Mentasty et al., 1999). UOP's Oleflex process (Bhasin et al., 2001) and CB&I Lummus's Catofin process (Craig and Spence,

1986) have been developed and commercialized based on these two catalyst families. New catalyst formulations such as vanadium oxides (Eon et al., 1994; Khodakov et al., 1998), gallium oxides (Michorczyk and Ogonowski, 2003), and carbon-based catalysts (Qi and Su, 2014) are continuously explored to achieve better performance. Despite significant progress in catalytic PDH, a number of limitations exist, including catalyst deactivation, high cost, particularly on Pt, and environmental concerns associated with the use of heavy metals.

Recently, an experimental and kinetic modeling study on *n*-butane and *i*-butane pyrolysis at various pressures has shown that the branched structure of *i*-butane leads to a high propylene selectivity during pyrolysis (Li et al., 2018). However, only trace amount of butanes is available in shale deposits while propane can be obtained at around 1–2 mol% (Sattler et al., 2014b) Propane pyrolysis without any catalysts could be a simple approach to decompose propane for propylene production. However, high temperature (>700 ºC) is required to break the strong C–H and C–C bonds (410 and 370 kJ/mol, respectively) (Hidaka et al., 1989; Layokun and Slater, 1979; Zou and Zou, 1986), leading to significantly low propane conversion without the use of catalysts. In addition, the lower dissociation energy of the C–C bonds than that of the C–H bonds results in low propylene selectivity from propane pyrolysis than that from catalytic propane dehydrogenation. One possible approach to improve propylene yields from propane pyrolysis is to accelerate the cleavage of the C–H bonds. This could be achieved using catalysts or by providing additional free radicals as hydrogen abstraction agents so that the formation of propyl radicals, the precursors leading to propylene, is more favorable. It is well known in combustion chemistry that hydroxyl radicals can abstract hydrogen from alkanes to accelerate the formation of alkenes (Tuazon et al., 2003; Tully et al., 1986a; Droege and Tully, 1986b; Altarawneh et al. 2011). In atmospheric chemistry, alkoxy radicals are also known to abstract

hydrogen atoms from alkanes to produce alkenes (Zhao et al., 2003; Francisco et al., 2002; Griller and Ingold, 1974; Paul et al., 1978). However, these radicals are also very reactive towards the produced alkenes, eventually oxidizing them into carbon dioxide. As a result, the yields of alkenes in these reaction systems are typically low.

The ideal candidate radicals for accelerating propane conversion into propylene should be more reactive in abstracting hydrogen atoms from propane than from propylene. In this work, phenyl radicals generated from nitrobenzene were examined as a hydrogen abstraction agent in propane pyrolysis to accelerate the formation of propylene. Nitrobenzene was chosen to generate phenyl radicals because its low C–N bond energy (295.8 kJ/mol), compared to higher C–H bond energy (472.2 kJ/mol) in benzene, C–C bond energy (426.8 kJ/mol) in toluene, and C–O bond energy (463.6 kJ/mol) in phenol (Luo and Kerr, 2012). A plug flow reactor operated at a temperature range between 550–650 ºC was used for this reaction. The effect of nitrobenzene partial pressure and reaction temperature on propane pyrolysis was investigated. A detailed kinetic model was also used for the interpretation of the experimental results. The results obtained from this exploratory work could lead to future applications of any easily generated free radicals in hydrocarbon pyrolysis for the enhancement of conversion and manipulation of product yields.

2 Experimental Methods

2.1 Pyrolysis Reaction

Propane pyrolysis experiments were carried out in a continuous plug flow reactor between 550 ºC and 650 ºC at atmospheric pressure. The reactor consists of a quartz tube with a length of 11 in., an outer diameter of 0.5 in., and an inner diameter of 0.375 in. The quartz tube was placed in a furnace with a heating zone of 9.0 in. in length. A type-K thermocouple (OMEGA,

KMQSS-062U-12) was positioned in the middle of the reactor to monitor the reaction temperature. Propane (Airgas, 99%) was introduced through a gas line with a length of 13 in. at a flow rate between 0–35 ml/min. Nitrogen (Airgas, 99.998%) was used as a balance and carrier gas so that the total flow rate stayed constant at 53.5 ml/min. The propane and nitrogen flow rates were controlled by flow meters (Porter VCD-1000). Nitrobenzene (Acros Organics, 99%) was delivered by a syringe pump (KD Scientific) through a liquid line with a flow rate between 9.25–37.5 μL/min. Both gas and liquid lines were heated by heating tapes (McMaster-Carr, 4550T133) at a constant temperature of 250 ºC. Propane and nitrobenzene vapor were mixed before being fed into the reactor. The products of every 15 minute interval were collected in two ice–salt traps at –30 ºC downstream of the reactor and analyzed by gas chromatography (GC). The average values of 4 time-on-stream data (i.e., over a period of 1 hour) were reported in the figures, and the standard deviation of the 4 runs was used as error bars.

2.2 Products identification and quantification

Identification of the reaction products was achieved using a Shimadzu GC2010 Plus GC equipped with a mass spectrometer (MS). The samples were injected into the GC/MS system equipped with a Shimadzu SH-RXi-5Sil MS column (30 m). High purity helium (99.999%, Airgas) was used as a carrier gas in the column with a constant flow rate of 88.8 mL/min. The inlet temperature of the GC was set at 285 ºC. The programmed temperature regime for the GC oven was: start at 35 ºC, hold for 7 minutes, ramp up to 185 ºC at 7.5 ºC/min, and ramp up to 285 ºC at 20 ºC/min. The temperature of the MS detector was set at 285 ºC.

Quantification of the reaction products was achieved using a Shimadzu GC2010 Plus GC with a flame ionization detector (FID). The samples were injected into the GC/FID system equipped with a Shimadzu Rxi-5ms column (15 m). The GC was programmed with the

following inlet operating parameters: high purity helium carrier gas set at a constant flow pressure of 22.1 kPa, inlet temperature set at 285 ºC, and split injection mode with split ratio of 150. The detector temperature was set at 285 ºC, with an air flow rate of 400 mL/min, a hydrogen gas flow rate of 40 mL/min, and a makeup gas flow rate of 30 ml/min. The GC oven was programmed with the following temperature regime: start at 35 ºC, hold for 7 minutes, ramp up to 87.5 ºC at 7.5 ºC/min and hold for 2 minutes, ramp to 185 ºC at 7.5 ºC/min, and ramp to 285 ºC at 20 ºC/min. To determine the flow rates of NO and NO_2 in the product stream, atomic balances of nitrogen and oxygen were performed assuming that the loss of nitrobenzene mass in the product stream solely consisted of nitrobenzene derived products detected by FID and undetectable NO and NO_2. Since two atomic balance equations (one for nitrogen and one for oxygen) could be set up for each experiment, the two unknown quantities (i.e., NO and NO_2 flow rates in the product stream, respectively) could be readily solved.

Yields and selectivity of propane–derived products are calculated on per carbon basis as:

$$Yield\ (\%) = \frac{n_i F_i}{\sum_i n_i F_i + 3F_{C_3H_8}} \times 100\ \% \qquad (1)$$

$$Selectivity\ (\%) = \frac{n_i F_i}{\sum_i n_i F_i} \times 100\ \% \qquad (2)$$

where n_i and F_i are number of the carbon atoms and molar flow rate of the propane-derived product *i*, respectively. Similarly, yields of nitrobenzene–derived product *j* are calculated on per mass basis as:

$$Yield\ (\%) = \frac{m_j}{\sum_j m_j + m_{nitrobenzene}} \times 100\ \% \qquad (3)$$

where m_j is the mass flow rate of nitrobenzene-derived product *j* and $m_{nitrobenzene}$ is the mass flow

rate of unreacted nitrobenzene in the product stream.

2.3 Kinetic Modeling

To elucidate the reaction pathways in detail, kinetic modeling of the reaction system was performed. The Lawrence Livemore *n*-heptane combustion mechanism (Curran et al., 1998), which contains 654 species and 2,827 reactions, was used to describe the pyrolysis of the light hydrocarbons.. For reactions related to nitrobenzene, 4 reactions involving 5 additional species were added, as tabulated in Table 1. Specifically, Reaction 1 describes the cleavage of C–N bond of nitrobenzene to form phenyl and NO_2 radicals. The frequency factor (A) and activation energy (E_a) of the reaction were obtained from Gonzalez et al. (1985). Reactions 2 and 3 depict hydrogen abstraction from propane by phenyl radicals to form normal propyl radicals (n-C_3H_7) and isopropyl radicals (i-C_3H_7), respectively. The activation energies of the reactions were set based on Park et al. (2004). Representative frequency factor for hydrogen abstraction reactions is set following the recommendation by Kruse et al. (2001). Reaction 4 describes decomposition of NO_2 radicals to form NO, with parameters obtained from the GRI-Mech 3.0 methane combustion mechanism with NO_x chemistry (Smith et al., 1999). Note that the parameters used in the kinetic model were entirely obtained or estimated from the literature without fitting the experiment data. The final reaction mechanism used for the simulations in this work consists of 659 species and 2,831 reactions, which is provided in the Appendix along with the thermodynamic data of the species.

Plug Flow Reactor Module in ANSYS Chemkin 17.0 was used to simulate our experimental setup. This module is suitable for modeling the gas flow in the quartz reactor, since the flow in the quartz reactor is laminar, with a very small Reynolds number of ~1.22. Consequently, the hydrodynamic entry length is estimated to be 0.023 in. and the thermal entry

length is estimated to be 0.016 in, both of which are much smaller than the length of the heated zone (9 in.) of the quartz reactor. Since our experiments were conducted at a constant temperature, the simulations assumed that the whole process was isothermal instead of adiabatic and the endothermic effects of propane pyrolysis were assumed to be unimportant.

Table 1 Parameters in reactions involved with phenyl radicals[1]

	Reaction	A (mol-cm-sec-K)	n	E_a (cal/mol)	Reference
1	$C_6H_5NO_2 = C_6H_5 + NO_2$	3.16×10^{15}	0	6.83×10^{4}	Gonzalez et al. (1985)
2	$C_6H_5 + C_3H_8 = n\text{-}C_3H_7 + C_6H_6$	1.5×10^{11}	0	3.85×10^{3}	Park et al. (2004)
3	$C_6H_5 + C_3H_8 = i\text{-}C_3H_7 + C_6H_6$	1.5×10^{11}	0	3.85×10^{3}	Kruse et al. (2001)
4	$NO + O + M = NO_2 + M$	1.06×10^{20}	-1.41	0	Smith et al. (1999)

[1]Rate constant following the equation: $k(T) = AT^n \exp(-\frac{Ea}{RT})$

3 Results and Discussion

Fig. **1** depicts the effect of reaction temperature on product distributions for neat and phenyl facilitated propane pyrolysis. At 550 ºC, the conversion of neat propane pyrolysis reached only approximately 3% (Fig. 1A). When the reaction temperature increased to 600 and 650 ºC, the conversion increased to approximately 5% and 15%, respectively. Propylene had the highest selectivity at approximately 45% regardless temperature examined (Fig. 1B). When propane pyrolysis was facilitated by phenyl radials, the conversion of propane was significantly higher, reaching approximately 15% at 550 ºC, 25% at 600 ºC, and 35% at 650 ºC, respectively. Methane, ethylene, and propylene were found as the major products and their yields all increased in the presence of nitrobenzene compared to neat pyrolysis. The selectivity of propylene in phenyl radical facilitated pyrolysis, however, decreased from approximately 50% to approximately 30% at 550 ºC in favor of methane and ethylene. The same decrease in

propylene selectivity in favor of methane and ethylene was also observed at 600 and 650 ºC.

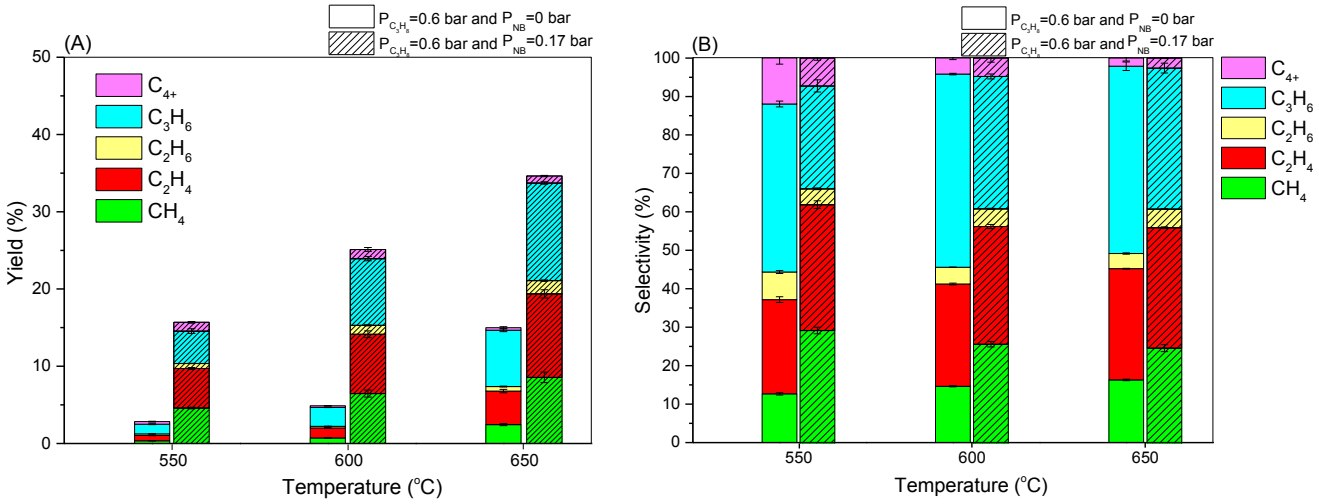

Fig. 1. Temperature dependence of propane pyrolysis with or without the addition of phenyl radicals.

Fig. 2 compares rate constants of the three propane pyrolysis initialization reactions. Reaction A is the cleavage of propane C–C bonds to produce C_2H_5 and CH_3 radicals. Reactions B and C are the cleavage of C–H bonds to produce *n*-C_3H_7 and *i*-C_3H_7 radicals, respectively (along with H radicals). The rate constants (*k*) of all three reactions increased with increasing temperature, consistent with the temperature effect on propane conversion shown in Fig. 1. The rate constant of C–C bond cleavage (Reaction A) was higher than that of C–H bond cleavage (Reactions B and C) regardless of the temperature. This suggests that C–C bond cleavage is the more dominant initialization reaction in propane pyrolysis. The produced C_2H_5 and CH_3 radicals from Reaction A can further abstract hydrogen from propane to form *i*-C_3H_7 and *n*-C_3H_7 radicals, which are the precursors for propylene. In the presence of additional hydrogen abstracting radicals, such as phenyl radicals, the formation of *i*-C_3H_7 and *n*-C_3H_7 radicals is dramatically accelerated. As illustrated in Fig. 2, hydrogen abstraction from propane using phenyl radicals has a much lower activation energy (Reaction D), meaning that temperature has

little effect. This explains the increase in propane conversion and propylene yields in phenyl facilitated propane pyrolysis.

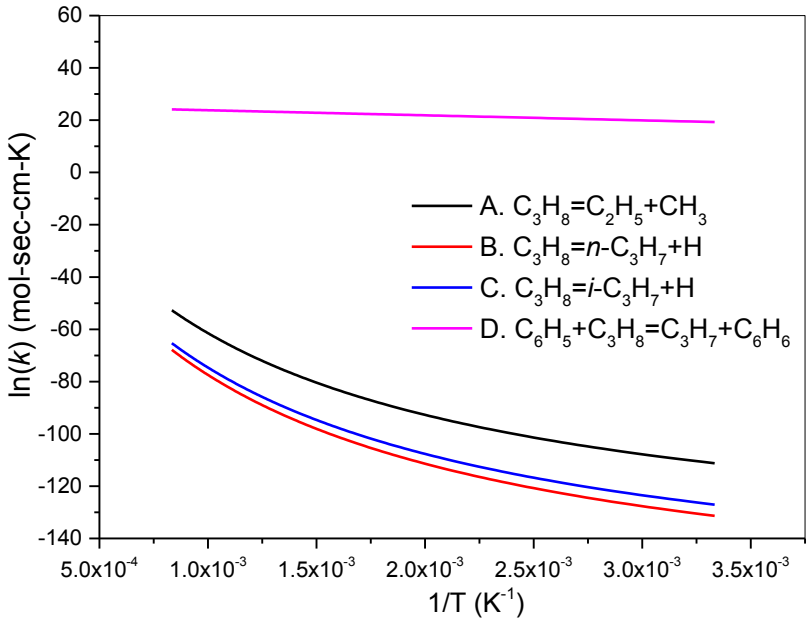

Fig. 2. Comparison of rate constants (Curran et al., 1998) of three different propane pyrolysis initialization reactions: C–C bond cleavage (A), C–H bond cleavage (B and C), and hydrogen abstraction by phenyl radicals (D) reaction.

The effect of nitrobenzene partial pressure on product yields and selectivities at 600 ºC is shown in Fig. 3. In our experiments, nitrobenzene partial pressure was varied between 0–0.17 bar. Propane partial pressure was kept constant at 0.6 bar and inert nitrogen was used as the balance gas so that the total pressure was constant at 1 atm. Our results showed that the yields of all products (Fig. 3A) increased with increasing nitrobenzene partial pressure. This can be explained by the fact that more phenyl radicals were produced with increasing nitrobenzene partial pressure, which resulted in higher concentration of *n*-C_3H_7 and *i*-C_3H_7 radicals and increased product yields. However, the selectivity of propylene was found to decrease with increasing nitrobenzene partial pressure in favor of ethylene and methane (Fig. 3B). This trend is agreeable with the modeling results, shown as curves in the figures. To gain a fundamental

understanding of the origin of increased propane conversion yet decreased propylene selectivity, flux analyses of the reactions involving major products (C_2H_4, CH_4, C_3H_6) was conducted.

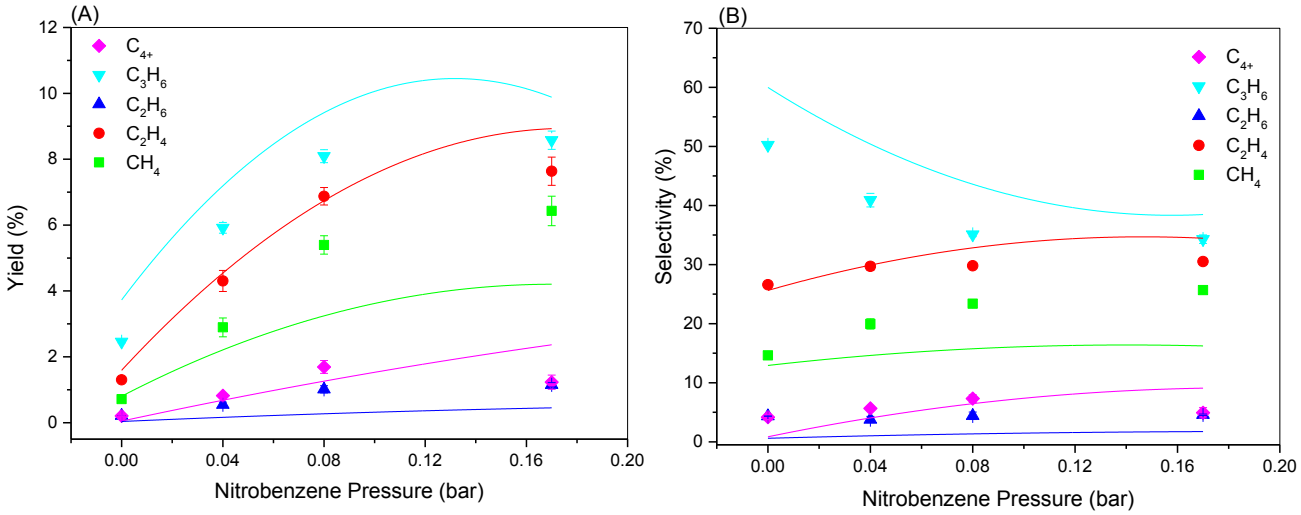

Fig. 3. The effect of nitrobenzene pressure on (A) the yields and (B) species selectivity of phenyl facilitated propane pyrolysis. Symbols represent experimental data, and the curves represent simulation results.

Fig. 4 shows the model predicted major fluxes associated with the reactions involving ethylene production at the end of the reactor. All reaction rates increased with the presence of phenyl radicals. The model suggests that *n*-C_3H_7 radicals account for 86% and 77% of the formation of ethylene in neat and phenyl facilitated propane pyrolysis, respectively. Since the formation of *n*-C_3H_7 radicals was accelerated by the presence of phenyl radicals, the additional production of *n*-C_3H_7 radicals in phenyl facilitated propane pyrolysis resulted in increased ethylene yields. The second most dominant reaction pathway leading to ethylene formation is decomposition of propylene assisted by hydrogen radicals, with methyl radicals (CH_3) as the second product. This explains why the decreased selectivity of propylene in phenyl facilitated propane pyrolysis was accompanied by increased selectivity of ethylene and methane.

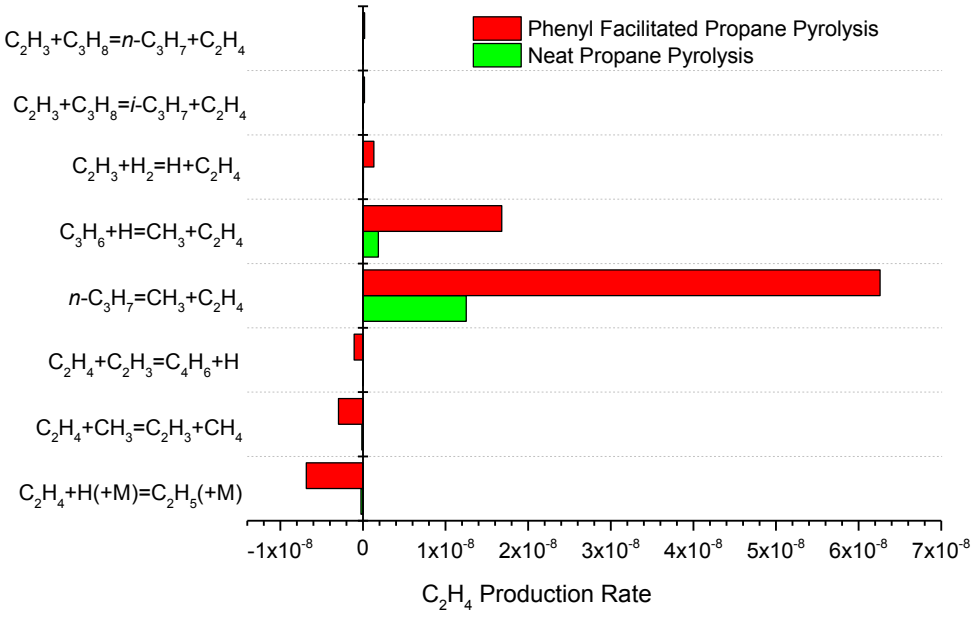

Fig. 4. Model predicted reaction rates for C_2H_4 production in phenyl facilitated propane pyrolysis and neat propane pyrolysis.

Model predicted fluxes of reactions involving methane production at the end of reactor are shown in Fig. 5. It can be seen that all reaction rates are positive, suggesting that no reactions consume CH_4 due to its stability. Increased concentration of phenyl radicals in phenyl facilitated propane pyrolysis results in increased CH_4 yields. Moreover, CH_4 formation is exclusively through CH_3 radicals, part of which is produced from propylene (second reaction in Fig. 5). This explains that increased propane conversion in the presence of phenyl radicals led to increased methane selectivity and decreased propylene selectivity in our experiments.

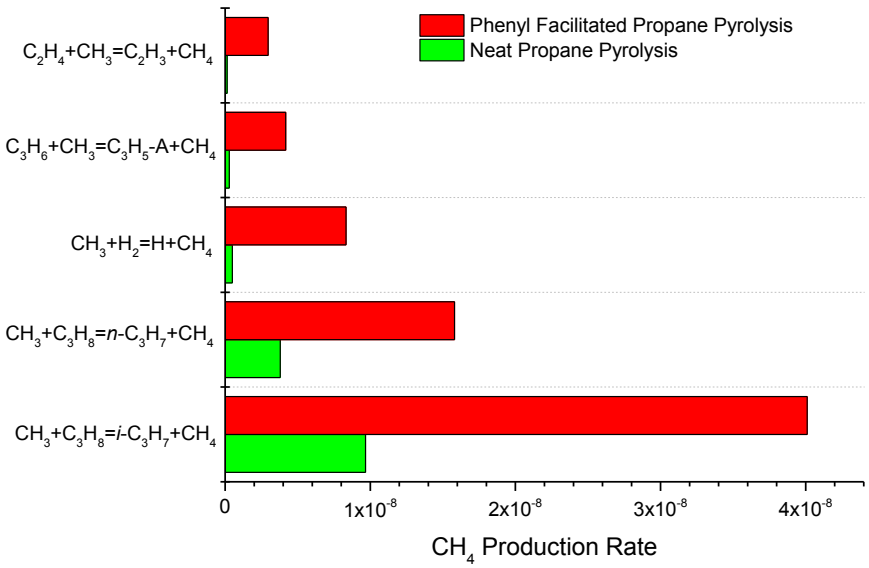

Fig. 5. Model predicted reaction rates for CH_4 production in phenyl facilitated propane pyrolysis and neat propane pyrolysis.

Fig. 6 shows model predicted fluxes of reactions involving propylene production in neat and phenyl facilitated propane pyrolysis. The reaction rates in phenyl facilitated propane pyrolysis all increase due to higher radical concentrations. The primary radical to produce C_3H_6 is *i*-C_3H_7, which also consumes propylene to form C_3H_8 and allyl (C_3H_5-A) radicals. However, the model suggests that about 65% of the C_3H_5-A radicals convert back to C_3H_6, with the remaining 35% lead to the production of molecules C_4 or larger. Neglecting the reaction pathways involving C_3H_5-A, Fig. 6 shows that the major pathways responsible for the net consumption of C_3H_6 are the production of C_2H_4 and CH_3 radicals, which explains the increased selectivity of ethylene and methane and decreased selectivity of propylene in the presence of phenyl radicals in our experiments.

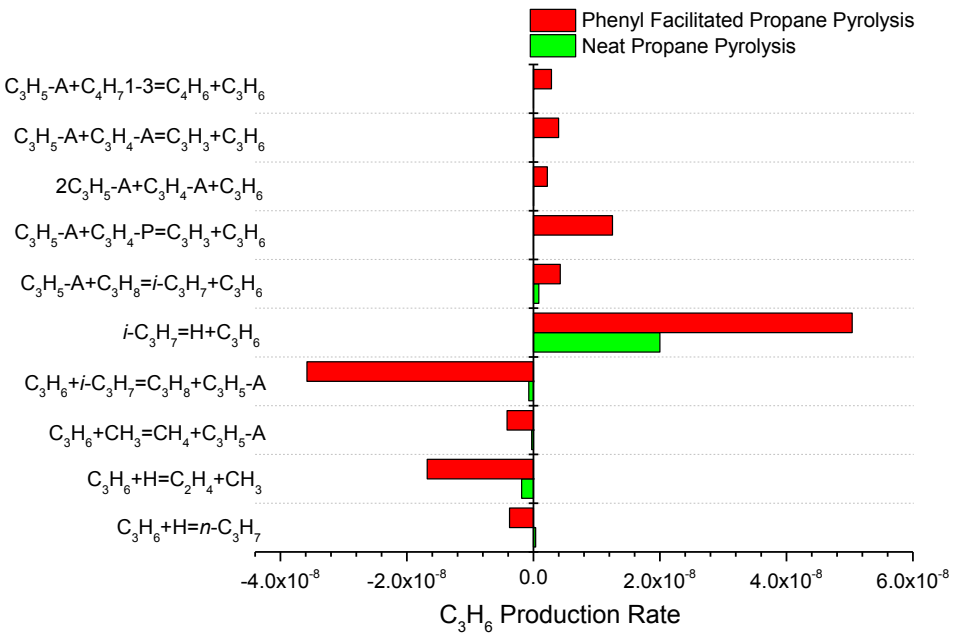

Fig. 6. Model predicted reaction rates for C_3H_6 production in phenyl facilitated propane pyrolysis and neat propane pyrolysis.

Based on the above flux analyses, major reaction pathways of phenyl facilitated propane pyrolysis are sketched in Fig. 7. The initialization of propane pyrolysis involves either C–C bond breakage to form CH_3 and C_2H_5 radicals or C–H bond breakage to form H and *n*-C_3H_7 or *i*-C_3H_7 radicals. The radicals formed from the initialization reactions can further abstract hydrogen atoms from propane to produce *n*-C_3H_7 and *i*-C_3H_7 radicals. When the phenyl radicals produced from nitrobenzene are present, they can abstract hydrogen atoms from propane much more easily, which accelerates the formation of *n*-C_3H_7 and *i*-C_3H_7 radicals (red arrows). Although *n*-C_3H_7 radicals can be converted into propylene, they mainly decompose into C_2H_4 and CH_3 radicals that lead to CH_4 (blue arrows). Both *n*-C_3H_7 and *i*-C_3H_7 radicals lead to the production of C_3H_6 (green arrows), which can be partly converted into C_2H_4 and CH_3 radicals (pink arrow) and C_4 hydrocarbons via allyl (C_3H_5-A) radicals. Overall, this reaction mechanism suggests that the decreased propylene selectivity in phenyl facilitated propane pyrolysis is due

to the increased rates of secondary reactions converting C_3H_6 into C_2H_4 and CH_4, a result of increased concentrations of *n*-C_3H_7 and *i*-C_3H_7 radicals.

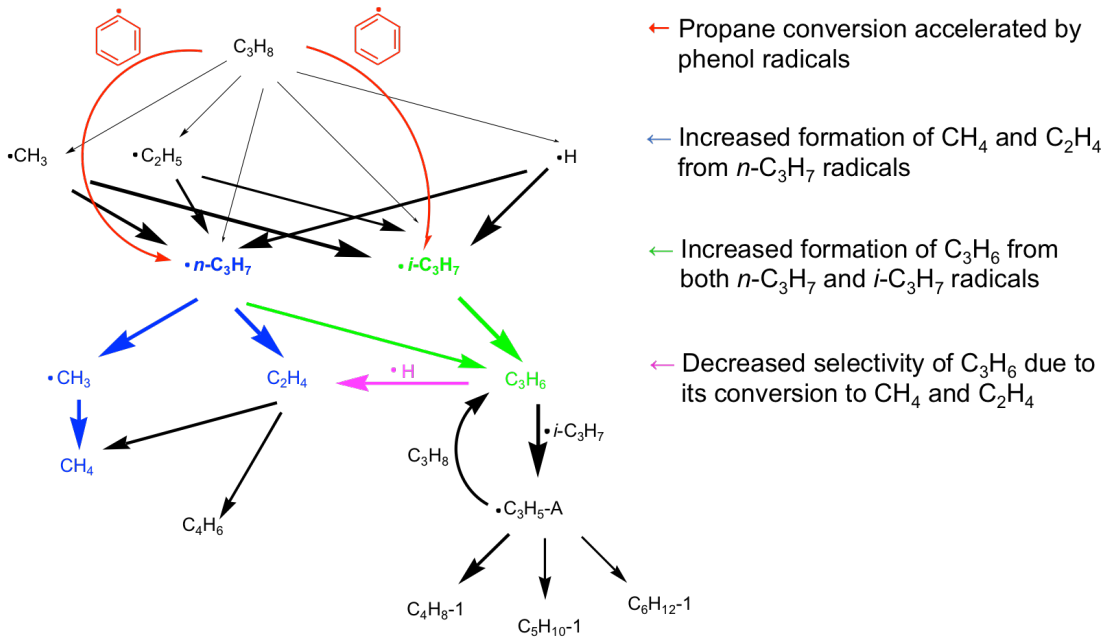

Fig. 7. Reaction pathways of phenyl facilitated propane pyrolysis.

Fig. 8 shows the yields of nitrobenzene-derived products in the presence or without the presence of propane during pyrolysis. Increased reaction temperature has a positive effect on nitrobenzene conversion and product yields. Phenol, benzene, NO_2, and NO were found as the major products, which were produced from nitrobenzene pyrolysis. The mechanism of forming these products is discussed in McCarthy and O'Brien (1980). Specifically, the direct cleavage of aromatic-nitrogen bonds gives NO_2 and phenyl radicals leading to benzene via subsequent hydrogen abstraction. On the other hand, the rearrangement of the atoms of a nitro group produces an aromatic-oxygen bond instead of an aromatic-nitrogen bond. This atom rearrangement initiates the removal of NO from the nitro groups and produces phenoxyl radicals, which lead to phenol via subsequent hydrogen abstraction. Minor products including

indole, diphenylamine, benzonitrile, and propylbenzene were found with yields lower than 1%, which are not shown in Fig. 8. Coupling products from nitrobenzene and propane, such as ethylbenzene, toluene and styrene, were also found, suggesting the existence of free radical recombination between nitrobenzene-derived phenyl radicals and propane-derived hydrocarbon radicals. These reactions, however, were not included in our kinetic model for simplicity due to their relatively low reaction rates, which were found to only contribute to less than 1% reduction in methane, ethylene, and propylene yields.

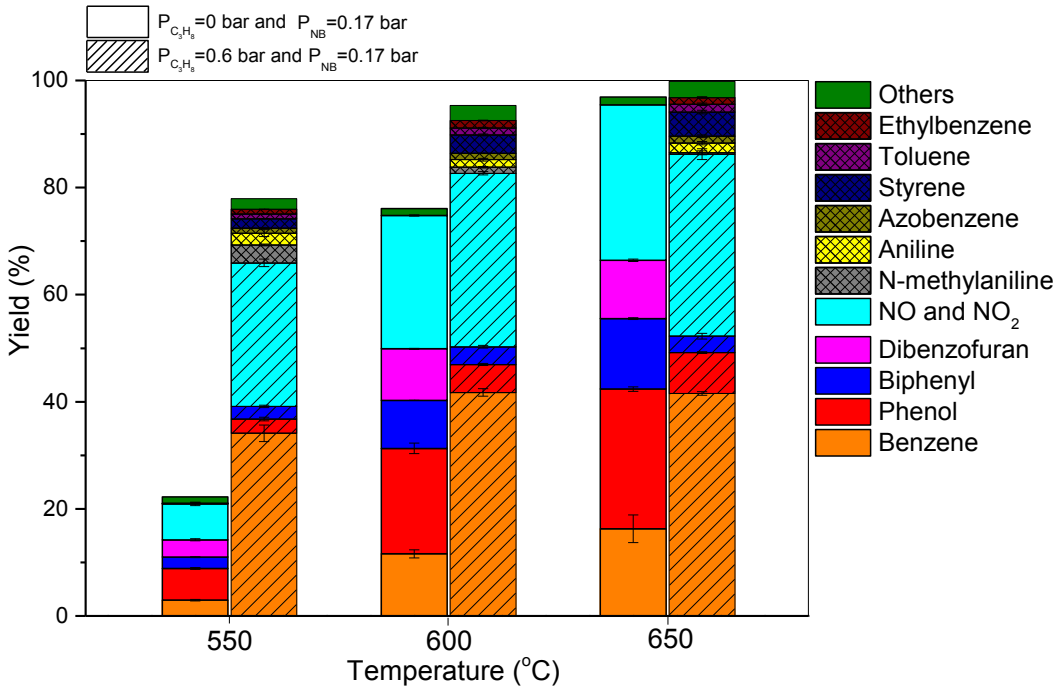

Fig. 8. The yields of nitrobenzene-derived products suggest temperature effect on the copyrolysis of nitrobenzene and propane.

4 Conclusions

Neat propane pyrolysis and pyrolysis facilitated by phenyl radicals were performed in a plug flow reactor with a temperature range between 550 ºC and 650 ºC. The results showed that propane conversion and products yields all increased in the presence of phenyl radicals. Higher

nitrobenzene partial pressure resulted in higher propane conversion and product yields. However, decreased propylene selectivity in favor of ethylene and methane was observed. The results from kinetic modeling agreed well with experiments results, and it is suggested that higher concentrations of *i*-C_3H_7 and *n*-C_3H_7 radicals were produced in phenyl facilitated propane pyrolysis. The increase in *n*-C_3H_7 radical concentrations led to increased formation of ethylene and methane, and the increase in *i*-C_3H_7 radical concentrations led to increased formation of propylene. However, higher concentrations of *n*-C_3H_7 and *i*-C_3H_7 radicals also led to accelerated secondary reactions converting C_3H_6 into C_2H_4 and CH_4 and decreased propylene selectivity. Our work demonstrates that in the presence of a suitable radical, propane conversion could be enhanced and propylene yields could be increased. The balance between increased propylene yields and decreased propylene selectivity, however, remains a major challenge.

Acknowledgements

Funding supports from the National Science Foundation (CBET-1842101) and UMass Lowell Faculty Startup Funds are greatly appreciated.

References

Altarawneh, M., Al-Muhtaseb, A.A.H., Dlugogorski, B.Z., Kennedy, E.M., Mackie, J.C., 2011. Rate constants for hydrogen abstraction reactions by the hydroperoxyl radical from methanol, ethenol, acetaldehyde, toluene, and phenol. Journal of Computational Chemistry 32, 1725-1733.

Bhasin, M., McCain, J., Vora, B., Imai, T., Pujado, P., 2001. Dehydrogenation and oxydehydrogenation of paraffins to olefins. Applied Catalysis A: General 221, 397-419.

Bruijnincx, P.C., Weckhuysen, B.M., 2013. Shale gas revolution: An opportunity for the production of biobased chemicals? Angewandte Chemie International Edition 52, 11980-11987.

Craig, R., Spence, D., 1986. Catalytic dehydrogenation of liquefied petroleum gas by the Houdry Catofin and Catadiene processes. Handbook of Petroleum Refining Process, 4-3.

Curran, H.J., Gaffuri, P., Pitz, W.J., Westbrook, C.K., 1998. A comprehensive modeling study of n-heptane oxidation. Combustion and Flame 114, 149-177.

Deng, L., Shishido, T., Teramura, K., Tanaka, T., 2014. Effect of reduction method on the activity of Pt–Sn/SiO_2 for dehydrogenation of propane. Catalysis Today 232, 33-39.

Droege, A.T., Tully, F.P., 1986b. Hydrogen atom abstraction from alkanes by hydroxyl. 5. n-Butane. The Journal of Physical Chemistry 90, 5937-5941.

Eon, J., Olier, R., Volta, J., 1994. Oxidative dehydrogenation of propane on γ-Al_2O_3 supported vanadium oxides. Journal of Catalysis 145, 318-326.

Francisco, C.G., Freire, R., Herrera, A.J., Peréz-Martín, I., Suárez, E., 2002. Intramolecular 1, 5-versus 1, 6-hydrogen abstraction reaction promoted by alkoxy radicals in carbohydrate models. Organic Letters 4, 1959-1961.

Gonzalez, A.C., Larson, C.W., McMillen, D.F., Golden, D.M., 1985. Mechanism of decomposition of nitroaromatics. Laser-powered homogeneous pyrolysis of substituted nitrobenzenes. The Journal of Physical Chemistry 89, 4809-4814.

Griller, D., Ingold, K., 1974. Abstraction of the hydroxylic hydrogen of alcohols by alkoxy radicals. Journal of the American Chemical Society 96, 630-632.

Hidaka, Y., Oki, T., Kawano, H., 1989. Thermal decomposition of propane in shock waves. International Journal of Chemical Kinetics 21, 689-701.

Jibril, B., 2004. Propane oxidative dehydrogenation over chromium oxide-based catalysts. Applied Catalysis A: General 264, 193-202.

Kerr, R.A., 2010. Natural gas from shale bursts onto the scene. American Association for the Advancement of Science.

Khodakov, A., Yang, J., Su, S., Iglesia, E., Bell, A.T., 1998. Structure and properties of vanadium oxide-zirconia catalysts for propane oxidative dehydrogenation. Journal of Catalysis 177, 343-351.

Kruse, T.M., Woo, O.S., Broadbelt, L.J., 2001. Detailed mechanistic modeling of polymer degradation: application to polystyrene. Chemical Engineering Science 56, 971-979.

Layokun, S.K., Slater, D.H., 1979. Mechanism and kinetics of propane pyrolysis. Industrial & Engineering Chemistry Process Design Development 18, 232-236.

Lee, M.-H., Nagaraja, B.M., Lee, K.Y., Jung, K.-D., 2014. Dehydrogenation of alkane to light olefin over PtSn/θ-Al_2O_3 catalyst: Effects of Sn loading. Catalysis Today 232, 53-62.

Li, W., Wang, G., Li, Y., Li., T., Zhang, Y., Cao, C., Zou, J., Law, C.K., 2018. Experimental and kinetic modeling investigation on pyrolysis and combustion of *n*-butane and *i*-butane at

various pressures. Combustion and Flame 191, 126-141.
Luo, Y.-R., Kerr, J., 2012. Bond dissociation energies. CRC Handbook of Chemistry Physics 89, 89.
McCarthy, E., O'Brien, K., 1980. Pyrolysis of nitrobenzene. Journal of Organic Chemistry 45, 2086-2088.
Mentasty, L.R., Gorriz, O.F., Cadus, L.E., 1999. Chromium oxide supported on different Al_2O_3 supports: Catalytic propane dehydrogenation. Industrial & Engineering Chemistry Research 38, 396-404.
Michorczyk, P., Ogonowski, J., 2003. Dehydrogenation of propane to propene over gallium oxide in the presence of CO_2. Applied Catalysis A: General 251, 425-433.
National Academies of Sciences, E., Medicine, 2016. The Changing Landscape of Hydrocarbon Feedstocks for Chemical Production: Implications for Catalysis: Proceedings of A Workshop. National Academies Press.
Nawaz, Z., 2015. Light alkane dehydrogenation to light olefin technologies: A comprehensive review. Reviews in Chemical Engineering 31, 413-436.
Park, J., Wang, L., Lin, M., 2004. Kinetics of phenyl radical reactions with propane, n-butane, n-hexane, and n-octane: Reactivity of C_6H_5 toward the secondary C-H bond of alkanes. International Journal of Chemical Kinetics 36, 49-56.
Paul, H., Small Jr, R., Scaiano, J., 1978. Hydrogen abstraction by tert-butoxy radicals. A laser photolysis and electron spin resonance study. Journal of the American Chemical Society 100, 4520-4527.
Qi, W., Su, D., 2014. Metal-free carbon catalysts for oxidative dehydrogenation reactions. ACS Catalysis 4, 3212-3218.
Sattler, J.J., Gonzalez-Jimenez, I.D., Luo, L., Stears, B.A., Malek, A., Barton, D.G., Kilos, B.A., Kaminsky, M.P., Verhoeven, T.W., Koers, E.J., Baldus, M., Weckhuysen, B.M., 2014a. Platinum-promoted Ga/Al_2O_3 as highly active, selective, and stable catalyst for the dehydrogenation of propane. Angewandte Chemie International Edition 53, 9251-9256.
Sattler, J.J., Ruiz-Martinez, J., Santillan-Jimenez, E., Weckhuysen, B.M., 2014b. Catalytic dehydrogenation of light alkanes on metals and metal oxides. Chemical Reviews 114, 10613-10653.
Sattler, J.J., Ruiz-Martinez, J., Santillan-Jimenez, E., Weckhuysen, B.M., 2014c. Catalytic dehydrogenation of light alkanes on metals and metal oxides. Chem Rev 114, 10613-10653.
Smith, G.P., Golden, D.M., Frenklach, M., Moriarty, N.W., Eiteneer, B., Goldenberg, M., Bowman, C.T., Hanson, R.K., Song, S., Gardiner, Jr. W.C., Lissianski, V.V., Qin, Z., 1999, GRI-Mech 3.0. http://www.me.berkeley.edu/gri_mech/.
Schweitzer, N.M., Hu, B., Das, U., Kim, H., Greeley, J., Curtiss, L.A., Stair, P.C., Miller, J.T., Hock, A.S., 2014. Propylene hydrogenation and propane dehydrogenation by a single-site Zn^{2+}on silica catalyst. ACS Catalysis 4, 1091-1098.
Stevens, P., 2012. The shale gas revolution: Developments and changes. Chatham House London.
Tuazon, E.C., Aschmann, S.M., Nguyen, M.V., Atkinson, R., 2003. H-atom abstraction from selected C-H bonds in 2, 3-dimethylpentanal, 1, 4-cyclohexadiene, and 1, 3, 5-cycloheptatriene. International Journal of Chemical Kinetics 35, 415-426.
Tully, F.P., Droege, A.T., Koszykowski, M., Melius, C.F., 1986a. Hydrogen-atom abstraction from alkanes by hydroxyl. 2. Ethane. The Journal of Physical Chemistry 90, 691-698.

Wang, Q., Chen, X., Jha, A.N., Rogers, H., 2014. Natural gas from shale formation–the evolution, evidences and challenges of shale gas revolution in United States. Renewable and Sustainable Energy Reviews 30, 1-28.

Wittcoff, H.A., Reuben, B.G., Plotkin, J.S., 2004. Industrial Organic Chemicals Second Edition. Chapter 4, 168.

Zhang, Y., Zhou, Y., Shi, J., Zhou, S., Sheng, X., Zhang, Z., Xiang, S., 2014. Comparative study of bimetallic Pt-Sn catalysts supported on different supports for propane dehydrogenation. Journal of Molecular Catalysis A: Chemical 381, 138-147.

Zhao, J., Zhang, R., North, S.W., 2003. Oxidation mechanism of δ-hydroxyisoprene alkoxy radicals: Hydrogen abstraction versus 1, 5 H-shift. Chemical Physics Letters 369, 204-213.

Zou, R., Zou, J., 1986. On interaction between ethane and propane in simultaneous pyrolysis and its influence on ethylene selectivity. Industrial & Engineering Chemistry Process Design Development 25, 828-834.